opposite long bond (carborane) nor short bond (cyclobutene, benzocyclobutenes) generates much distortion in the sp^3–sp^3 bond of the four-membered ring is inescapable.

Acknowledgment. This work was supported by the National Science Foundation through Grants CHE 83-18345, CHE 8617590, and CHE 8800448. We thank the Department of the Army for a generous gift of decaborane and Professors R. A. Pascal and J. E. Jackson for many helpful discussions.

Supplementary Material Available: Tables of atomic coordinates, H atom coordinates and thermal parameters, and anisotropic thermal parameters (2 pages); a table of observed and calculated structure factors (8 pages). Ordering information is given on any current masthead page.

Contribution from the Department of Chemistry, Stanford University, Stanford, California 94305, Department of Inorganic Chemistry, University of Sydney, NSW 2006, Australia, and Department of Chemistry, University of Michigan, Ann Arbor, Michigan 48109

Low-Temperature X-ray Absorption Spectroscopy of Plastocyanin: Evidence for Copper-Site Photoreduction at Cryogenic Temperatures

James E. Penner-Hahn,[†] Mitsuo Murata,[‡] Keith O. Hodgson,*[,§] and Hans C. Freeman[‡]

Received May 3, 1988

X-ray absorption spectra for copper(II) plastocyanin have been measured at low temperature. These data confirm our previous observation (based on room-temperature measurements) that the methionine sulfur in plastocyanin makes no significant contribution to the Cu EXAFS and that the Cu-S(Met) interaction must therefore be extremely weak. We report both preliminary data, having a very poor signal/noise ratio, and subsequent measurements with much higher quality data. Analysis of the preliminary data provides a cautionary example of the dangers of deriving structural results from noisy EXAFS data, at least in cases where the scatterer is weakly contributing to the signal. Analysis of the near-edge structure gives direct evidence for X-ray-induced photoreduction of Cu(II) when extremely intense X-rays from synchrotron sources are used. The rate of photoreduction decreases by approximately a factor of 2 between 190 and 4 K, but it is still significant even at the lower temperatures studied.

Introduction

Plastocyanin is a copper-containing electron-transfer protein. The copper atom is in a "type 1" or "blue" site characterized by an intense electronic absorption band at ~600 nm, an unusually small hyperfine splitting in the $g_{\parallel}$ region of the EPR spectrum, and an unusually high reduction potential.[1] The molecular structures of four "blue" Cu proteins—plastocyanin from poplar leaves,[2] two azurins (from *Pseudomonas aeruginosa*[3a,b] and *Alcaligenes denitrificans*[3c,d]), and the "basic blue protein" from cucumbers[4]—are now known from X-ray crystallographic studies. In the oxidized [Cu(II)] state of all four proteins the Cu atom is coordinated by the N atoms of two histidine residues, a cysteine S atom, and a methionine S atom. A refinement of the poplar plastocyanin crystal structure at 1.6 Å resolution has shown that the metal–ligand distances in this protein are Cu–N(His) = 2.04 and 2.10 Å, Cu–S(Cys) = 2.13 Å, and Cu–S(Met) = 2.90 Å, respectively, with esd's of ~0.05 Å.[5]

Although the unique features of blue Cu proteins have been substantially rationalized in terms of the X-ray structural results, the significance of the extremely long Cu–S(Met) bond remains a subject for speculation and study.[6] Polarized electronic absorption spectra and EPR spectra of oriented single crystals have shown that the S(Met) atom has at best a small effect on the ligand field at the Cu atoms.[7] Further, the S(Met) atom makes no significant contribution to the Cu extended X-ray absorption fine structure (EXAFS) of either plastocyanin[8] or azurin[9] in solution at room temperature. Understanding this result is important, in view of the widespread use of EXAFS spectroscopy in investigations of metalloprotein structure.[10]

Previously we reported EXAFS measurements on oriented single crystals of plastocyanin.[11] The orientations of the four symmetry-related molecules in the unit cell (Figure 1) are such that all the Cu–S(Met) bonds may be aligned parallel to the polarization vector (**c**||ê) or perpendicular to it (**b**||ê). In the **c**||ê orientation, the contribution of Cu–S(Met) to the EXAFS is expected to be enhanced by a factor of approximately 3. In the **b**||ê orientation, the contribution of the S(Met) to the Cu EXAFS is essentially zero.[10f] The single-crystal study confirmed, with greater sensitivity than was possible in the solution measurements, that the S(Met) makes no detectable contribution to the Cu EXAFS spectrum at room temperature.

The failure of the EXAFS measurements to detect a ligand of Cu whose presence had been demonstrated by the crystal structure analysis was explained in terms of thermal disorder.[11] Since the temperature parameters of the Cu and S(Met) atoms as determined by X-ray diffraction are relatively small,[5] the hypothesis of large thermal disorder in the EXAFS can be correct only if the vibrations of the Cu and S(Met) atoms are effectively uncorrelated.[11] If this is the case, then it should be possible to reduce the vibrational effects, and thus to enhance the EXAFS contribution of the S(Met) atom, by lowering the temperature

* To whom correspondence should be addressed.
[†] University of Michigan.
[‡] University of Sydney.
[§] Stanford University.

(1) Gray, H. B.; Solomon, E. I. In *Copper Proteins*; Spiro, T. G., Ed.; Wiley-Interscience: New York, 1981; Chapter 1.
(2) Colman, P. M.; Freeman, H. C.; Guss, J. M.; Murata, M.; Norris, V. A.; Ramshaw, J. A. M.; Venkatappa, M. P. *Nature* **1978**, *272*, 319-324.
(3) (a) Adman, E. T.; Stenkamp, R. E.; Sieker, L. C.; Jensen, L. H. *J. Mol. Biol.* **1978**, *123*, 35-37. (b) Adman, E. T.; Jensen, L. H. *Isr. J. Chem.* **1981**, *21*, 8-12. (c) Norris, G. E.; Anderson, B. F.; Baker, E. N. *J. Mol. Biol.* **1983**, *165*, 501-521. (d) Norris, G. E.; Anderson, B. F.; Baker, E. N. *J. Am. Chem. Soc.* **1986**, *108*, 2784-2785.
(4) Guss, J. M.; Merritt, E. A.; Phizackerley, R. P.; Hedman, B.; Murata, M.; Hodgson, K. O.; Freeman, H. C. *Science* **1988**, *241*, 806-811.
(5) Guss, J. M.; Freeman, H. C. *J. Mol. Biol.* **1983**, *169*, 521-563.
(6) (a) Freeman, H. C. In *Coordination Chemistry 21*; Laurent, J. P., Ed.; Pergamon Press: Oxford, England, 1981; pp 29-51. (b) Guss, J. M.; Harrowell, P. R.; Murata, M.; Norris, V. A.; Freeman, H. C. *J. Mol. Biol.* **1986**, *192*, 361-387.
(7) Penfield, K. W.; Gay, R. R.; Himmelwright, R. S.; Eickman, N. C.; Norris, V. A.; Freeman, H. C.; Solomon, E. I. *J. Am. Chem. Soc.* **1981**, *103*, 4382-4388.
(8) Tullius, T. D. Ph.D. Thesis, Stanford University, 1979.
(9) Tullius, T. D.; Frank, P.; Hodgson, K. O. *Proc. Natl. Acad. Sci. U.S.A.* **1978**, *75*, 4069-4073.
(10) (a) Scott, R. A. *Methods Enzymol.* **1985**, *117*, 414-459. (b) Powers, L. *Biochim. Biophys. Acta* **1982**, *683*, 1-38. (c) Lee, P. A.; Citrin, P. H.; Eisenberger, P.; Kincaid, B. M. *Rev. Mod. Phys.* **1981**, *53*, 769-806. (d) Teo, B. K. *Acc. Chem. Res.* **1980**, *13*, 412-419. (e) Cramer, S. P.; Hodgson, K. O. *Prog. Inorg. Chem.* **1979**, *25*, 1-39. (f) Hahn, J. E.; Hodgson, K. O. In *Inorganic Chemistry: Toward the 21st Century*; Chisholm, M. H., Ed.; ACS Symposium Series No. 211; American Chemical Society: Washington, DC, 1983; pp 431-444. (g) Cramer, S. P. In *X-ray Absorption*; Koningsberger, D. C., Prins, R. Eds.; Wiley: New York, 1988; pp 257-320.
(11) Scott, R. A.; Hahn, J. E.; Doniach, S.; Freeman, H. C.; Hodgson, K. O. *J. Am. Chem. Soc.* **1982**, *104*, 5364-5369.

0020-1669/89/1328-1826$01.50/0

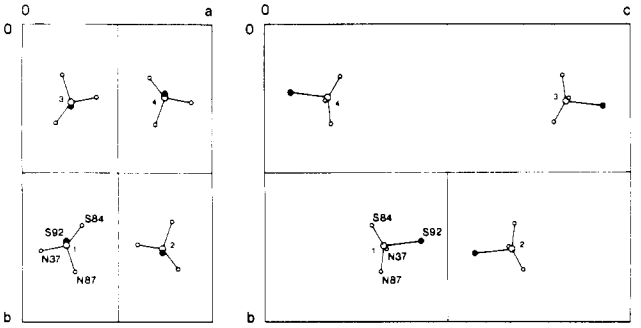

Figure 1. Projections of the unit cell of poplar plastocyanin. The Cu sites of the four symmetry-related molecules are shown enlarged by a factor of 2. N37 = N of His37, S84 = S of Cys84, N87 = N of His87, and S92 = S of Met92. The coordinates of the symmetry-related molecules, indicated by small numerals, are (1) x, y, z, (2) $^1/_2 + x, ^1/_2 - y, 1 - z$, (3) $^1/_2 - x, 1 - y, ^1/_2 + z$, and (4) $1 - x, ^1/_2 + y, ^1/_2 - z$. Left: Projection on the *ab* plane (*c* axis points away from reader). Right: Projection on the *bc* plane (*a* points toward the reader). The orientation having the *ab* plane perpendicular to the polarization vector gives the maximum sensitivity to the Cu–S92 EXAFS.

at which the measurements are made. In order to test this hypothesis, we have recorded EXAFS data for poplar copper(II) plastocyanin at a series of temperatures between 220 and 4 K, using both oriented single crystals (at 205 and 175 K) and frozen solutions (at 220, 190, 120, and 4 K). The analysis and results of these studies are reported herein.

Experimental Section

XAS Measurements. Plastocyanin from leaves of *Populus nigra* var. *italica* was purified and crystallized as previously described.[2,5] Four sets of measurements, two utilizing single crystals and two utilizing frozen solutions, were made. All X-ray absorption data were collected at the Stanford Synchrotron Radiation Laboratory (SSRL) under dedicated operating conditions (3.0 GeV, 40–80 mA). The spectra were measured as fluorescence excitation spectra by using from 1 to 20 NaI(Tl) scintillation detectors to monitor the Cu$K\alpha$ fluorescence.[12] Ni filters were used to reduce the background intensity for the solution measurements; no filters were necessary for single-crystal measurements, since the amount of background scattering was found to be small. The size of the incident beam was 2 × 20 mm for the solution measurements and 2 × 2 mm for the single-crystal measurements.

For the single-crystal measurements, the crystals were mounted in thin-walled glass capillaries together with a drop of mother liquor. The capillary was surrounded by a double-walled Mylar cell[13] of a design adapted from that described by Bartunik and Schubert.[14] Initial cooling of the crystals was complete in less than 5 min. The temperature of the inner chamber of the cell was regulated by adjusting the flow of a stream of dry nitrogen at liquid-N_2 temperature. The temperature at the crystal was taken to be the temperature of the N_2 gas leaving the inner chamber, as monitored with an iron–constantan thermocouple. Condensation of moisture was prevented by passing a stream of dried nitrogen at ambient temperature through the outer jacket of the cell and by blowing a stream of warm air over the entire apparatus.

The crystals were oriented with the aid of X-ray precession photographs prior to the XAS measurements. The orientations were checked in a similar manner after the XAS measurements. In all cases, the crystals continued to diffract strongly despite the exposure to X-radiation and despite fluctuations of the temperature during experimental setup.

The XAS data collection conditions are summarized in Table I. Initial low-temperature single-crystal measurements (data set I) utilized a bending magnet beam line (II-2) in an unfocused configuration. The Cu fluorescence was monitored by using a single 7.5 × 7.5 cm^2 NaI(Tl) detector. One crystal (no. 1) was used to record data (24 scans) for the **b**||**ê** orientation [Cu–S(Met) bond perpendicular to **ê**] at 205 K. A second crystal (no. 2) was used to record data (18 scans) for the **c**||**ê** orientation [Cu–S(Met) bond parallel to **ê**] at 175 K. The orientations of the Cu–S(Met) bond are described with reference to the crystal structure at room temperature (see Figure 1).

The same beam line, with a focusing mirror in place, was used for the initial low-temperature solution measurements (data set II). The sample

Table I. Low-Temperature XAS Data for Poplar Plastocyanin (in Chronological Order)

data set	specimen	temp, K	orientn	beam line	no. of scans
I	cryst 1	205	**b**||**ê**	II-2	24
	cryst 2	175	**c**||**ê**	II-2	18
II	frozen soln 1	220 (±10)		II-2	6
		120		II-2	10
III	cryst 3	175	**b**||**ê**	VI-2	9
	cryst 4	175	**c**||**ê**	VI-2	14
	cryst 5	175	**c**||**ê**	VI-2	10
		175	**b**||**ê**	VI-2	6
IV	frozen soln 2	4		VII-3	14
		190		VII-3	7

(ca. 10 mM Cu(II) plastocyanin in sodium phosphate buffer at pH 6.0) was sealed inside a vacuum-tight chamber, which was cooled by circulating liquid N_2 through its metallic base. The chamber was kept under vacuum during the experiment, and the temperature was monitored with an iron–constantan thermocouple in contact with the cell. The vacuum in the chamber was not perfect, and the resulting thermal conduction prevented the achievement of liquid-N_2 temperature at the specimen. Six scans were made at 220 ± 10 K, and 10 scans, at 120 K. The Cu fluorescence was monitored with an array of four 7.5 × 7.5 cm^2 NaI(Tl) detectors.

Since the initial low-temperature measurements (data sets I and II) suffered from high noise levels (see below), we collected additional data using wiggler beam lines and an array of 20 5 × 5 cm^2 NaI(Tl) detectors. The second set of low-temperature single-crystal measurements (data set III) were done by using the 54-pole wiggler beam line (VI-2, 8.9 kG) with a high cutoff-energy focusing mirror in place. Experimental equipment was equivalent to that described above, although improved cryostat construction permitted the temperature to be held nearly constant at 175 K. Three crystals (crystals 3–5) were used to record **b**||**ê** spectra (crystal 3, 9 scans; crystal 5, 6 scans) and **c**||**ê** spectra (crystal 4, 14 scans; crystal 5, 10 scans).

The second set of low-temperature solution measurements (data set IV) were made by using an eight-pole wiggler beam line (VII-3, 18 kG) in an unfocused configuration. The sample cryostat was of a double-jacketed design, in which the sample was placed in a Mylar-windowed Lucite cell,[13] which was in turn placed in a cold He environment. An outer vacuum jacket provided thermal isolation for the He chamber. The spectra of a single solution were measured at 4 and 190 K.[15]

Data Reduction and Analysis. Energy calibration was by means of a Cu foil internal standard[11] with the first inflection point of the Cu foil defined as 8980.3 eV. For each scan, the output from each detector (for data sets I and II) or the weighted-average output of the detectors (for data sets III and IV) was examined to ensure the absence of spurious signals. A weighted average[12] of all acceptable data was then calculated to produce the spectra reported herein. The preedge region (8670–8970 eV) of each average scan was fitted with a polynomial, and this background was subtracted from the data. Normalization of the edge spectra was accomplished by fitting a straight line to the postedge region (9045–9600 eV) and adjusting the scale so that the extrapolated value of the normalization line was 1.0 at 9000 eV.

Data were converted from an energy scale to a k scale by using the equation $k = [2m_e(E - E_0)/\hbar]^{1/2}$, with E_0 defined as 9000 eV. The EXAFS was calculated from the preedge-subtracted scans using a two- or three-region cubic spline to model the smooth background above the edge.[16] The spline points were adjusted to minimize the amplitude of the low-R (<1 Å) features in the Fourier transform without affecting the amplitude of the higher frequency EXAFS oscillations. In all cases, the Fourier transforms were insensitive to the details of the splines used in calculating the EXAFS, thus demonstrating that the results reported below are not artifacts of the data reduction procedure.

The Fourier transforms of the k^3-weighted EXAFS data were calculated by numerical integration. Some of the EXAFS plots (below) have been drawn with k^2 weighting to reduce the effects of noise. Quantitative analysis of the EXAFS data was accomplished by using a nonlinear least-squares curve-fitting procedure. The parametrized amplitude and phase function appropriate to a given absorber–scatterer pair were determined empirically as described previously[11,16] by using Cu(imidazole)$_4$(NO$_3$)$_2$ as a standard for Cu–N and Cu(diethyldithiocarbamate)$_2$ as a standard for Cu–S. The model was least-squares fitted to Fouri-

(12) Cramer, S. P.; Scott, R. A. *Rev. Sci. Instrum.* **1981**, *52*, 395–399.
(13) Mylar is a registered trademark of E. I. du Pont de Nemours & Co., Inc.
(14) Bartunik, H. D.; Schubert, P. *J. Appl. Crystallogr.* **1982**, *15*, 227–231.
(15) The Oxford Instruments CF1208 cryostat generously lent by Dr. S. P. Cramer was used.
(16) Co, M. S. Ph.D. Thesis, Stanford University, 1983.

Table II. Curve-Fitting Results for Data Sets III and IV

sample	data set	N		S		S′		
		N^a	R^b	N^a	R^b	N^a	$R^{b,c}$	F^d
				Frozen Solutions				
4 K	IV	4.3	2.00	0.5	2.08			0.48
		4.3	2.00	0.5	2.07	0.7	3.10	0.31
190 K	IV	3.2	1.98	0.6	2.16			0.65
		3.2	1.98	0.6	2.16	0.8	3.10	0.43
				Single Crystals				
cryst 3 (**b**||ê)	III	5.8	1.94	0.5	2.11			0.87
		5.9	1.94	0.5	2.11	0.5	3.11	0.82
cryst 4 (**c**||ê)	III	1.8	2.01	0.7	2.07	*e*		0.34
cryst 5 (**c**||ê)	III	1.0	2.02	0.5	2.08	*e*		0.12
cryst 5′ (**b**||ê)	III	3.0	1.95	0.5	2.20			0.90
		2.0	1.95	0.5	2.20	0.7	3.12	0.81

[a] Number of atoms in shell. [b] Absorber–scatterer distance. [c] R values for S′ were refined by starting from Cu–S′ = 2.9 Å. Alternative minima were observed for Cu–S′ = 2.7 Å. When Cu–S′ was constrained to be 2.9 Å, the S′ coordination number refined to a negative value. In all cases, a better fit could be obtained by including a shell of carbon atoms with Cu–C = ~3.0 Å instead of the Cu–S′ shell (i.e., the S′ "minima" arise from fitting the imidazole C EXAFS with the Cu–S EXAFS wave). [d] $F = [\chi(\text{calc}) - \chi(\text{obs})]^2k^6/(N - 1)$, where N is the number of data points. [e] Attempts to include an S′ shell significantly perturbed the fitting results for N and S. No stable Cu–S′ minimum was observed near 2.9 Å. [f] This crystal exhibited substantial radiation damage (see text), thus accounting for the different structural parameters.

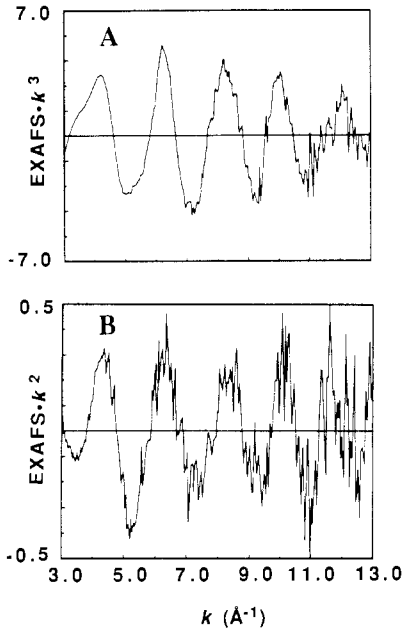

Figure 2. Representative EXAFS spectra for plastocyanin measured at low temperature: (A) data set IV measured at 4 K; (B) data set I, crystal 2, measured at 175 K. The plastocyanin crystal was oriented to maximize contribution of Cu–S(Met) to the EXAFS spectrum. In both cases, data are multiplied by k^n to enhance the sensitivity to high-k oscillations (n = 3 for data set IV and 2 for the noisier data set I). Note the difference in scale for solution relative to polarized EXAFS.

er-filtered EXAFS data by using a wide filter (typically 0.8–3.0 Å^{-1}) in order to avoid distorting the data. For the fits in Table II, σ_{vib} and E_0 were fixed at the same values as for the model compounds. Additional fits (not shown) where N was fixed and σ_{vib} varied gave equivalent results.

Results

EXAFS—Data Sets III and IV. An EXAFS spectrum typical of the data quality obtained in the data sets III and IV is shown in Figure 2A. The Fourier transforms for the data sets III and IV are shown in Figure 3. It is immediately obvious by looking at the Fourier transforms in the region between 2 and 3 Å that these data provide no dramatic evidence for an EXAFS contribution from the Cu–S(Met) interaction at low temperature. The features seen in this region are consistent with contribution from outer-shell imidazole atoms.[16] This qualitative interpretation is quantitatively supported by the curve-fitting analysis (Table II), which shows no improvement in the quality of the fit when a shell of sulfur is included either at the distance found in the Cu(II) plastocyanin crystal structure (2.9 Å) or at a normal copper–thioether distance (ca. 2.4 Å).

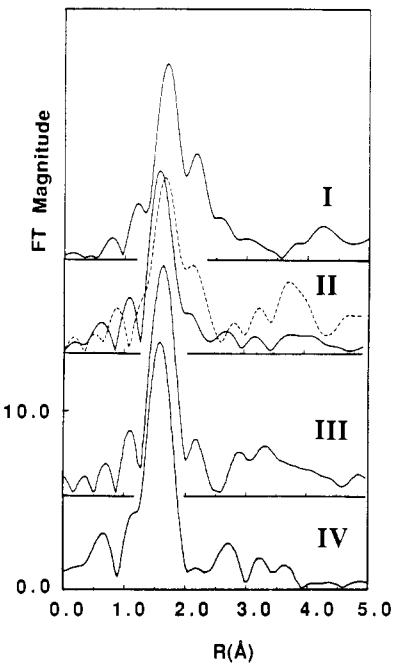

Figure 3. Fourier transforms of k^3-weighted EXAFS data. Data have been rescaled to give comparable FT magnitudes for each spectrum. Indicated scale is correct for data set IV. To convert this scale, multiply the other spectra by 0.7 (set I), 2.4 (set II), or 0.66 (set III). Transform ranges are indicated below in parentheses. The range was always ca. k = 3–13 Å^{-1}, with some modifications depending on the noise level of the data. Where possible, the FT end points were chosen as nodes in the EXAFS amplitude. Variation in the transform range affects low-R (<1 Å) background peaks but has no effect on peaks between 1.0 and 3 Å. Data set I: single crystal oriented to maximize the contribution of Cu–S(Met) to the EXAFS (3–13 Å^{-1}). Data set II (frozen solutions (3–13 Å^{-1})): data measured at 220 K (—); data measured at 120 K (---). Data set III: crystal 4, oriented to maximize contribution of Cu–S(Met) to EXAFS (3.8–12.12 Å^{-1}). Data set IV: frozen solution at 4 K (3.15–12.96 Å^{-1}).

Edge Structure—Data Sets III and IV. Examination of the edges reveals that one of the crystals and the frozen solution used to record data sets III and IV underwent a time-dependent photoreduction. While there have been several reports that metalloproteins, and in particular Cu proteins, can undergo photoreduction on exposure to intense X-ray beams,[17] we have not observed this phenomenon in our previous room-temperature

(17) Chance, B.; Angiolillo, P.; Yang, E. K.; Powers, L. *FEBS Lett.* **1980**, *112*, 178–182.

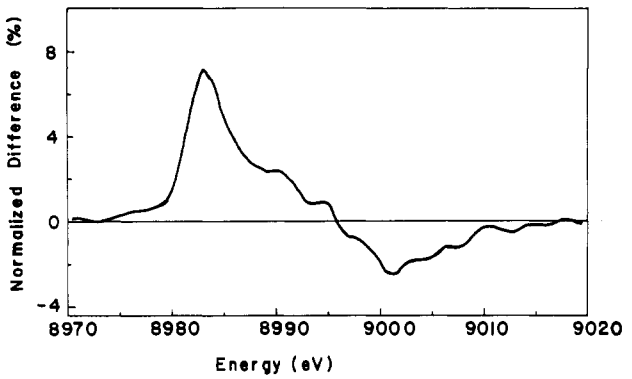

Figure 4. Normalized difference in absorption edge structure for data set IV, calculated for the last scan in set IV (scan 7 at 190 K) *minus* the first scan (scan 1 at 4 K). The ordinate is the percentage change relative to the total edge jump. The maximum at ca. 8984 eV indicates a greater amount of Cu(I) in the last scan relative to the first scan.

studies of poplar Cu(II) plastocyanin solutions[8] or single crystals.[11]

Radiation damage in copper proteins may be monitored by a number of techniques, including optical reflectance and EPR spectroscopy.[18] We have found that the large difference between the X-ray absorption edge structures of Cu(I) and Cu(II) provides a sensitive, convenient in situ method to determine the oxidation state of the sample during irradiation.[19-21] The normalized difference between two scans (e.g. first minus last) can be used to detect a change in oxidation-state composition of ca. 5%.[20] This approach proved to be of much value in analysis of the photoreduction effects observed in this study.

In the case of the single-crystal measurements (data set III), the photoreduction was so pronounced that we were able to observe bleaching of the blue color of crystal 5 during the attempted measurement of the **b**||**ê** spectra. This crystal had been used previously for measuring the **c**||**ê** spectra, and the color of the crystal had not changed visibly during those measurements. However, examination of the edge spectra for crystal 5 revealed that the formation of Cu(I) was significant during the recording of both the **c**||**ê** spectra and the **b**||**ê** spectra. In contrast with these observations, irradiation of crystal 3 (4 h) and crystal 4 (8 h) caused no spectral changes attributable to the formation of Cu(I).

Photoreduction also occurred during the solution measurements (data set IV). Aluminized Mylar cryostat windows precluded optical monitoring of the Cu oxidation state; however, edge structure could again be used for this purpose. Since the same solution was used to measure, sequentially, the 4 and 190 K data, a sensitive test for photoreduction was obtained by calculating the difference between the edge spectra recorded during the first 4 K scan and the last 190 K scan. The shape of this difference spectrum (Figure 4) is consistent with those observed for authentic (previously reported) Cu(I) minus Cu(II) difference spectra.[20-22] The amplitude of the peak at 8984 eV is proportional to the amount of Cu(I) present in the sample.[20] From comparison with model compounds,[21] the spectrum in Figure 4 corresponds overall to reduction of 10–15% of the Cu in the sample.

In order to determine the rate at which photoreduction occurred, difference spectra were calculated for the last 190 K scan minus every scan in data set IV. The amplitude of the 8984-eV difference peak as a function of scan number n is shown in Figure 5. The ordinate in this plot is proportional to the amount of Cu(I) produced between scan n and the final scan. Although an absolute

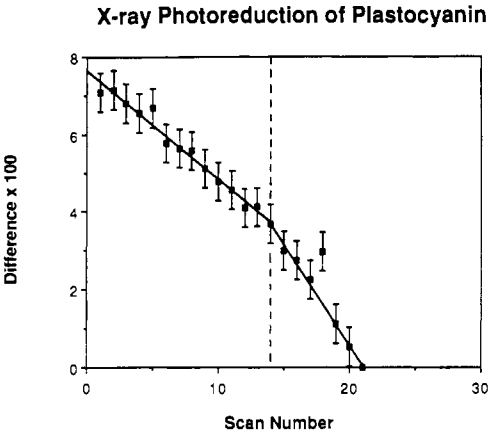

Figure 5. Amplitude of the difference edge peak at 8984 eV in data set IV. The ordinate is the magnitude of the difference peak at 8984 ± 1 eV for the last scan from set IV (scan 7 at 190 K) minus every other scan in set IV. Data were normalized to an edge jump of 1. The abscissa refers to sequential scans, with numbers 1–14 referring to scans at 4 K and numbers 15–20 referring to the first six scans at 190 K. Vertical bars indicate uncertainty in peak height due to statistical uncertainty and uncertainty in normalization. The vertical dashed line marks the temperature change from 4 to 190 K. Solid lines are the best straight-line fits to the data over the low- and high-temperature regimes.

time base is not available, the scan number is proportional to irradiation time and approximately proportional to elapsed time. A good fit to the data in Figure 5 is obtained by using a model that assumes a constant rate of Cu(I) production, with the rate dependent on temperature. The apparent rate of Cu(I) production doubles when the temperature is raised from 4 to 190 K.

The total elapsed time for 21 25-min scans was ca. 13 h, including a total irradiation time of ca. 9 h. The average incident X-ray flux was ca. 10^{11} photons/s, so that the sample received a total of 3×10^{15} photons. The irradiated sample volume was not more than 4×10^{-2} mL, giving, for a 10 mM sample, a total of ca. 0.01 X-ray photons/Cu(II) center. If 15% of the Cu(II) atoms were reduced (see above), an upper estimate of the photoreduction quantum yield is ca. 15 Cu(II) atoms/incident X-ray photon. This is well below the number of solvated electrons that should be produced by a single 9-keV photon.[23] As will be discussed in more detail below, the observed photoreduction does not affect in any significant way the results presented in Table II.

EXAFS—Data Sets I and II. Our initial series of measurements included the first X-ray absorption spectra ever recorded from oriented single crystals of a metalloprotein at low temperature. A typical EXAFS spectrum from these data sets is shown in Figure 2B. Despite the high noise level of the EXAFS, we attempted to proceed with data analysis. The Fourier transforms are shown in Figure 3. In contrast with antecedent room-temperature measurements, which had shown only a single resolvable shell of scatterers around the Cu,[11] the Fourier transforms of these low-temperature data showed two resolved peaks. This suggested the presence of two distinct shells of scatterers around the Cu in plastocyanin at low temperature. The new peak at 2.1 Å was consistent with a shell at ca. 2.4 Å. In the transforms of the solution data, the amplitude of the 2.1-Å peak increased with decreasing temperature. Such a marked temperature dependence would be expected for a weakly bonded ligand.[24] From the single-crystal data, it was clear that the 2.1-Å feature was observed only in the **c**||**ê** orientation. This is the orientation that, in the case of crystals at room temperature, samples the Cu–S(Met) EXAFS.[11]

(18) Powers, L.; Chance, B.; Ching, Y.; Angiolillo, P. *Biophys. J.* **1981**, *34*, 465–498.
(19) LuBien, C. D.; Winkler, M. E.; Thamann, T. J.; Scott, R. A.; Co, M. S.; Hodgson, K. O.; Solomon, E. I. *J. Am. Chem. Soc.* **1981**, *103*, 7014–7016.
(20) Hahn, J. E.; Co, M. S.; Spira, D. J.; Hodgson, K. O.; Solomon, E. I. *Biochem. Biophys. Res. Commun.* **1983**, *112*, 734–745.
(21) Kau, L.-S.; Spira-Solomon, D. J.; Penner-Hahn, J. E.; Hodgson, K. O.; Solomon, E. I. *J. Am. Chem. Soc.* **1987**, *109*, 6433–6442.
(22) Penner-Hahn, J. E.; Hedman, B.; Hodgson, K. O.; Spira, D. J.; Solomon, E. I. *Biochem. Biophys. Res. Commun.* **1984**, *119*, 567–574.
(23) For a dilute protein solution, the majority of the X-ray photons are absorbed by the oxygen in water. For a 9-keV photon, the resulting photoelectron will have substantial kinetic energy and is expected to produce numerous additional electrons through a cascade of secondary ionization processes. For an average ionization energy of 30 eV, as many as 300 photoelectrons could be produced.
(24) Eisenberger, P.; Brown, G. S. *Solid State Commun.* **1979**, *29*, 481–484.

Table III. Curve-Fitting Results for Data Sets I and II

sample	data set	N		S		S′		
		N^a	R^b	N^a	R^b	N^a	R^b	F^c
				Frozen Solutions				
220 K	II	4.4	2.03	1.4	2.08			1.00
		4.3	2.03	1.6	2.09	0.8	2.38	0.77
120 K	II	3.6	2.04	1.9	2.10			1.26
		1.9	2.10	3.2	2.13	1.6	2.39	0.80
				Single Crystals[d]				
295 K (**b**||ê)	I	4.1	1.98	1.3	2.08			1.28
		4.1	1.98	1.3	2.08	0.3	2.73	1.26
205 K (**b**||ê)	I	5.0	2.01	2.2	2.08			0.82
		4.5	2.02	2.4	2.09	0.4	2.37	0.78
295 K (**c**||ê)	I	0.6	2.04	0.6	2.10			0.77
		0.6	2.04	0.6	2.10	0.2	2.76	0.76
175 K (**c**||ê)	I	1.6	2.02	0.8	2.08			0.75
		0.4	2.05	1.4	2.11	0.9	2.37	0.53
				Crystal Structure Analysis[e]				
		2.0	2.07	1.0	2.13	1.0	2.90	

[a] Number of atoms in shell. [b] Absorber–scatterer distance. [c] $F = [\chi(\text{calc}) - \chi(\text{obs})]^2 k^6/(N-1)$, where N is the number of data points. [d] Results at ambient temperature are averages of data taken from ref 11. [e] From ref 5.

As has been noted briefly elsewhere,[25] there were at least two qualitative interpretations of these results: either the structure of plastocyanin changes at low temperature or the crystallographically determined room-temperature Cu–S(Met) distance (2.9 Å) in fact represents the weighted average of two conformers having respectively a short (ca. 2.4 Å) and a long (ca. 3.2 Å) Cu–S(Met) distance. The first interpretation seemed unlikely to be correct in the absence of any optical or EPR spectroscopic evidence to indicate temperature-dependent change at the Cu(II) site of plastocyanin.[26] In addition, X-ray edge structure (see below) also indicates *no* temperature-dependent structure changes.

The second interpretation implied that the $-CH_2-CH_2-S-CH_3$ side chain of residue Met92 can have two closely similar conformations. In one conformation the S^δ atom makes a contact of 2.4 Å with the Cu atom. In the other conformation the S^δ---Cu distance must be somewhat greater than 2.9 Å (say 3.1 Å). If the two S^δ sites contribute to the structure in proportion to their relative occupancies, they lead to the observation of a "weighted mean S^δ atom" at 2.9 Å from the Cu atom, i.e., at the position determined by X-ray crystal structure analysis at ambient temperature.[29]

In order to test the plausibility of this interpretation, calculations were undertaken to establish the conditions under which the presence of two conformers differing only with respect to the position of the Met92 side chain might have escaped detection during the crystal structure analysis of copper(II) plastocyanin. Using the original X-ray diffraction data at 1.6-Å resolution, it was possible to show that a 30% contribution by a conformer having its S(Met) atom at 2.4 Å from the Cu atom would certainly have been detected by the electron-density difference methods used in the structure analysis; a <30% contribution might not have been detected if there was no reason to suspect it. Details of the calculations will be published elsewhere.[30]

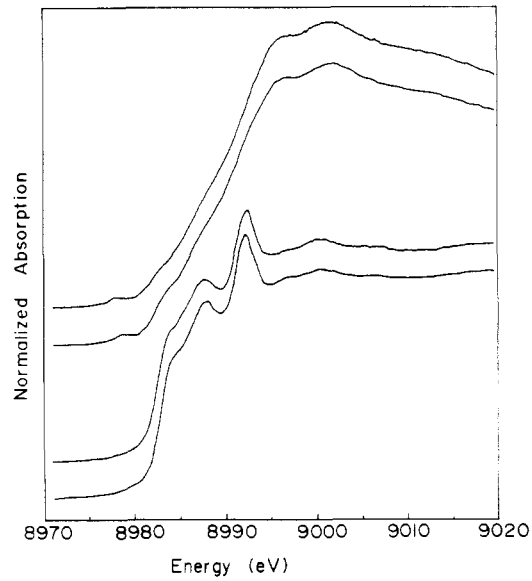

Figure 6. Room-temperature and low-temperature polarized plastocyanin absorption edge structure. For each pair, the upper spectrum was recorded at room temperature and the lower spectrum at low temperature (175 K). Top: Crystal oriented with **b**||ê (polarization perpendicular to Cu–S92 direction). Bottom: Crystal oriented with **c**||ê (polarization parallel to Cu–S92 direction).

Since the crystallographic calculations did not eliminate the hypothesis that a second conformer contributed <30% to the structure as described above, it was expected that a quantitative fit to the EXAFS would be obtained with a model having 2 N at 2.0 Å, 1 S at 2.1 Å and ~0.3 S at 2.4 Å from the Cu atom. The curve-fitting results were *not* consistent with this prediction (Table III). For the solution data (data set II), the sulfur shell at the long (2.4 Å) distance was clearly required to obtain a good fit to the data, and the amplitude of this shell increased as the temperature decreased, as expected. However, the amplitude of the shell corresponded to a structure in which the *majority* of the Cu sites had short (2.4 Å) Cu–S(Met) distances, particularly at 120 K. Such a structure was incompatible with the crystallo-

(25) Penner-Hahn, J. E.; Hodgson, K. O. In *Structural Biological Applications of X-ray Absorption, Scattering, and Diffraction*; Bartunik, H. D., Chance, B., Eds.; Academic Press: New York, 1986; pp 35–47.

(26) The formation of a weak Cu–S(Met) bond at low temperature is, however, among the effects that have been proposed to account for differences between the resonance Raman spectra of plastocyanin at ambient temperature and at 10–77 K.[27,28] Further testing of this hypothesis awaits a crystal structure analysis of Cu(II) plastocyanin at low temperature.

(27) Woodruff, W. H.; Norton, K. A.; Swanson, B. I.; Fry, H. A. *Proc. Natl. Acad. Sci. U.S.A.* **1984**, *81*, 1263–1267.

(28) Blair, D. F.; Campbell, G. W.; Schoonover, J. R.; Chan, S. I.; Gray, H. B.; Malmström, B. G.; Pecht, I.; Swanson, B. I.; Woodruff, W. H.; Cho, W.; English, A. M.; Fry, H. A.; Lum, V.; Norton, K. A. *J. Am. Chem. Soc.* **1985**, *107*, 5755–5766.

(29) It is well established that the crystallographic refinement of a protein structure at 1.6-Å resolution may not resolve two partially occupied atomic positions separated by only 0.5–0.7 Å and that the atoms in such positions are likely to behave as their weighted mean. For example, the crystal structure analysis of the reduced form of poplar plastocyanin at pH 5.9 did not resolve a mixed population of protonated and unprotonated molecules in which the positions of the Cu(I) atoms differ by about 0.7 Å. The apparent position of the Cu(I) atom at pH 5.9 was the weighted mean of the positions found independently in crystals of the protonated protein at pH 3.8 and the unprotonated protein at pH 7.8, respectively.[6]

(30) Church, W. B.; Freeman, H. C. Unpublished work.

graphic results. Further, the amplitudes of the Cu–N and short Cu–S shells at the short distance were too large by a factor of ~2. (In the absence of other inconsistencies, this might have been attributed to the decreased thermal damping at low temperature.)

Further contradictions were present in the single-crystal data (data set I). The room-temperature[11] and low-temperature curve-fitting results are compared in Table III. The amplitudes of the Cu–N and short Cu–S shells were again somewhat increased at low temperature. Consistent with Figure 3, the sulfur shell at the long (2.4 Å) distance made a significant contribution to the fit only for the c||ê orientation. The EXAFS amplitude for polarized experiments is expected to increase by a factor of 3 relative to isotropic measurements.[11] Thus, the observed Cu–S′ amplitude, 0.9, was much too small in comparison with the amplitude, 0.8–1.6, for this shell when fitted to the solution data. These inconsistencies, and the obviously high noise level of the initial data, were the reasons why we subsequently repeated these measurements using lower temperatures, higher flux beam lines, and a larger array of detectors, as described earlier (data sets III and IV).

Edge Structure—Data Sets I and II. No evidence for X-ray-induced photoreduction was observed in data sets I and II. There was no detectable change in the edge structure during the course of either the single-crystal or the solution measurements. The room-temperature[11] and low-temperature (data set I) polarized single-crystal edge spectra for copper(II) plastocyanin are compared in Figure 6. These spectra are virtually identical both for the b||ê and for the c||ê orientations. Since the polarized spectra for Cu(I) and Cu(II) plastocyanin are quite different,[31,32] this result shows that all four samples had the same average oxidation state. Given the widely different conditions under which these samples were prepared and irradiated, it seems unlikely that they would have had *identical* compositions with respect to oxidation state unless all four samples were fully oxidized.

The absence of photoreduction is intriguing. Since copper(I) plastocyanin is known to have a 2.5-Å Cu–S(Met) bond at low pH,[6] photoreduction would have been a plausible explanation for the apparent EXAFS contribution of a 2.4-Å Cu–S shell in data sets I and II. Clearly, this was not the case.

Discussion

Low-Temperature EXAFS. In our original report on poplar copper(II) plastocyanin EXAFS,[11] we suggested that the absence of any detectable contribution from S(Met92) to the Cu EXAFS was most probably due to essentially uncorrelated motion of the S(Met) relative to the Cu atom. This hypothesis would be confirmed if it were possible to freeze out this relative motion and thus to observe the Cu–S(Met) EXAFS at low temperature. The present work shows that there is no detectable contribution of Cu–S(Met) to the EXAFS, even at a temperature as low as 4 K (Figure 3 and Table II). The discrepancy between the final results from data sets III and IV, and the earlier suggestion[25] that there is a 2.4-Å Cu–S(Met) interaction in plastocyanin at low temperature, is now known to be due to the high noise level of data sets I and II. In retrospect, it is clear that the appearance of peaks in the Fourier transform and the ability to fit these peaks with a shell of atoms were invalid criteria for the quality of data sets I and II and that the true noise level was better indicated by the unreasonably high amplitudes which were obtained for the Cu–N and short Cu–S shells.

Expected Magnitude of Cu–S(Met) EXAFS Contribution. The absence of any Cu–S(Met) contribution even at 4 K makes it interesting to attempt a calculation of the expected effect. The Debye–Waller thermal damping factor for EXAFS data, σ_{vib}^2, can be expressed as

$$\sigma_{vib}^2 = \frac{h}{8\pi^2\mu\nu} \coth (h\nu/2kT) \qquad (1)$$

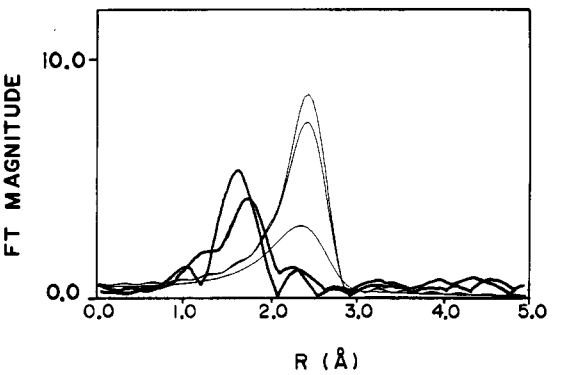

Figure 7. Fourier transforms for plastocyanin single crystals oriented with c||ê. All transforms were calculated by using k^3-weighted data over the range k = 4–12 Å^{-1}. Dark line: Observed transforms for two different plastocyanin crystals at room temperature (from ref 11). Light line: Transform for polarized EXAFS calculated by using "normal" and "weak" parameters for the Cu–S interaction (see text for definitions). In order of decreasing amplitude, calculations are for normal Cu–S at 4 K, normal Cu–S at room temperature, and weak Cu–S at 4 K. The calculated intensity for weak Cu–S decreases rapidly with increasing temperature and is not detectable at 175 K.

where μ is the reduced mass of the absorber–scatterer pair and ν is the absorber–scatterer vibrational frequency.[10d] In the absence of Cu(II)–S model compounds for which ν_{Cu-S} is known, a reasonable estimate of 314 cm^{-1} for "normal" Cu–S bonds can be obtained from Fe–S clusters.[33] Equation 1 gives $\sigma_{vib}^2 = 4.0 \times 10^{-3}$ Å^2 for "normal" Cu–S bonds at room temperature with this value decreasing to 2.5×10^{-3} Å^2 at 4 K. The Fourier transforms of the observed polarized EXAFS for copper(II) plastocyanin at room temperature and the calculated room-temperature EXAFS for a "normal" 2.9-Å Cu–S interaction (ν_{Cu-S} = 314 cm^{-1}) are compared in Figure 7.

In order to estimate the temperature dependence of the Cu–S(Met) EXAFS, we require the value of σ_{vib}^2(Cu–S). A reasonable lower estimate of σ_{vib}^2 can be obtained by using eq 1, with ν_{Cu-S} set to 50 cm^{-1}, the estimated upper limit for the Cu–S(Met) stretching frequency derived from resonance Raman measurements.[34] This gives $\sigma_{vib}^2 = 1.6 \times 10^{-2}$ Å^2 at 4 K, with this value increasing to 7.8×10^{-2} Å^2 at 175 K. The upper limit on σ_{vib}^2, corresponding to completely uncorrelated motion, is the sum of the individual atomic mean-square displacements (σ_{atomic}^2).[35] These displacements are not available for plastocyanin. However, a reasonable lower estimate may be obtained from Fe–S clusters, where both the Fe and the S have σ_{atomic}^2 values of ca. 0.057 Å^2[36] at room temperature. The EXAFS amplitudes calculated for this model are comparable to the "weak" interaction discussed above, provided one assumes that the pair-distribution function still obeys a Gaussian mode. From Figure 7, it is evident that the EXAFS for a "normal" Cu–S(Met) interaction should be readily detectable and that the EXAFS for a weak interaction (as defined above) might be detectable at 4 K. Note however that this interaction would probably only be detectable for polarized measurements at 4 K, since these have a 3-fold greater sensitivity to the Cu–S(Met) EXAFS and decreased interference from Cu–N_2S(Cys) EXAFS.[11] Unfortunately, it was only possible to measure *solution* data at 4 K. The calculated EXAFS for a weak Cu–S interaction at 175 K (the lowest temperature at which single-crystal measurements were made) has a negligible amplitude in comparison with the data shown in Figure 7. A further limitation on detectability of the Cu–S(Met) EXAFS is the fact that weak interactions are unlikely to be well described by the standard EXAFS formulation. In particular, the anharmonicity of such a weak bond would result in further distortion and decrease of the Fourier transform peak.

(31) Penner-Hahn, J. E.; Hedman, B.; Hodgson, K. O.; Freeman, H. C. Manuscript in preparation.
(32) Penner-Hahn, J. E. Ph.D. Thesis, Stanford University, 1984.
(33) Teo, B. K. *J. Am. Chem. Soc.* **1979**, *101*, 5624–5631.
(34) Frank, P. Personal communication.
(35) Böhmer, W.; Rabe, P. *J. Phys. C* **1979**, *12*, 2465–2474.
(36) Bunker, B.; Stern, E. A. *Biophys. J.* **1977**, *19*, 253–264.

These calculations, while obviously simplistic, indicate at least the order of magnitude of the possible effects. We conclude that, for atoms between which the "bonding" is extremely weak, it may not be possible to observe EXAFS oscillations even at liquid-He temperature. The negative result of the present work therefore does not eliminate the hypothesis that it was designed to test.

Temperature Independence of Absorption Edge Structure. New evidence for the weakness of the Cu–S(Met) interaction is provided by the fact that the copper(II) plastocyanin absorption edges at ambient and low temperatures are identical (Figure 6). The sensitivity of absorption edge structure, and in particular polarized edge structure, to the details of the molecular structure is well-known.[37] Since the thermal damping depends exponentially on k, the X-ray absorption signature of weakly bonded atoms will be strongest in the edge region, where k is small.[38] Thus, the most likely region in which to observe effects of the Cu–S(Met) interaction will be close to the edge. The fact that the edge structure is independent of temperature down to 4 K suggests that even at this temperature S(Met) does not make a significant contribution to the Cu X-ray absorption spectrum.

Photoreduction of Poplar Copper(II) Plastocyanin. Photoreduction of copper(II) plastocyanin was observed in two experiments: the polarized XAS measurements on crystal 5 at 175 K (data set III) and the XAS measurements on a solution in pH 6.0 sodium phosphate buffer at 4 and 190 K (data set IV). The observation that a high-flux X-ray beam can induce the photoreduction of a metalloprotein *even at 4 K* is the least expected result of the present work. It has hitherto been widely believed[10a] that very low temperatures decrease the rate of diffusion of solvated electrons sufficiently to inhibit photoreduction.

The lack of detectable photoreduction during the initial low-temperature measurements (data sets I and II), as well as during earlier measurements at ambient temperature,[11] is attributable to lower X-ray fluxes. The bending magnet sources for these data had ~10–20-fold lower fluxes than the wiggler beam lines VI-2 and VII-3 used for data sets III and IV. For the same photoreduction quantum yields as previously calculated, these fluxes would have caused negligible formation of Cu(I) during the course of the experiments.

Crystals 3–5 (data set III) were irradiated under identical conditions on the intense 54-pole wiggler beam line VI-2. A simple calculation leads to the expectation that the rates of photoreduction for the three crystals should have been of the same order as the rate of photoreduction of the solution in data set IV: although the volume was smaller for the crystal than for the solution, the concentration of Cu(II) atoms in the crystal (~0.09 M) was greater than in the solution (0.01 M); the numbers of atoms irradiated in the two sets of experiments must accordingly have been roughly the same. On the other hand, a decrease in photoreduction by a factor of only 5 would have reduced the amount of Cu(I) produced below 5%, the level of detectability. The failure to observe photoreduction in crystals 3 and 4 can thus be rationalized.

The question remains why, under apparently identical conditions of irradiation, crystal 5 was photoreduced to an extent where the blue color was visibly bleached, while crystals 3 and 4 were not. The only significant difference between the three experiments was that numerous interruptions—some as long as 18 h in duration—occurred during the data collection for crystal 5. During some of these interruptions, the crystal was allowed to return to ambient temperature. The extreme photoreduction presumably resulted from the increased rate of diffusion of the primary reductant (most likely solvated electrons) during the periods when the crystal was being neither cooled nor irradiated.

Effect of Photoreduction on EXAFS Measurements. The structural conclusions from the present work are unaffected by the occurrence of photoreduction in some of the experiments. As stated above, the extent of photoreduction during the collection of polarized EXAFS data from crystals 3 and 4 (data set III) was below the threshold of detectability (~5%). During the solution measurements at 4 K (data set IV), less than 10% of the Cu(II) was photoreduced. The average of the scans recorded at 4 K will thus closely reflect the structure of the Cu(II) site in poplar plastocyanin.

Conclusions

This work demonstrates that very intense X-ray beams can cause radiation damage in a redox-active metalloprotein even at 4 K. X-ray absorption edge structure is shown to be a convenient and sensitive in situ probe that monitors mixed Cu(I)/Cu(II) oxidation states. The observed radiation damage has implications for future X-ray absorption data collection, since it suggests a potential barrier to the effective utilization of the next generation of high-intensity synchrotron radiation sources. One solution to this problem will be to measure data by using many samples, each for a short period of time.

The XAS of poplar copper(II) plastocyanin exhibits no temperature dependence in the edge and EXAFS regions (except for the normal overall EXAFS amplitude increase at lower temperature). The observation of an EXAFS contribution from S(Met92) at low temperature would have confirmed the hypothesis[11] that the absence of such a contribution at ambient temperature is caused by dynamic disorder (i.e., a large Debye–Waller factor) and that the Cu–S(Met92) bond must, therefore, be weak. The absence of an EXAFS contribution from S(Met92) even at 4 K is consistent with this hypothesis but leaves it unconfirmed.

These results have important more general implications for EXAFS studies. The inability to clearly detect, even at 4 K, EXAFS oscillations due to an atom that is known to be present in the coordination sphere demonstrates one of the weaknesses of EXAFS. A negative EXAFS result does not *prove* that a particular scatterer is absent. The precise conditions under which an atom becomes (un)detectable by EXAFS remain to be determined, and this problem clearly merits further careful investigation.

Acknowledgment. This work was supported in part by National Science Foundation Grant CHE-8512129 (to K.O.H.) and by grants from the Australian Research Grants Scheme (C80/15377) and from ESSO Australia Ltd. (to H.C.F.). Synchrotron radiation beam time was provided by the Stanford Synchrotron Radiation Laboratory, which is supported by the U.S. Department of Energy, Office of Basic Energy Sciences, and the Division of Research Resources of the National Institutes of Health.

(37) Smith, T. A.; Penner-Hahn, J. E.; Berding, M. A.; Doniach, S.; Hodgson, K. O. *J. Am. Chem. Soc.* **1985**, *107*, 5945–5955.
(38) Bunker, G.; Stern, E. A. *Phys. Rev. Lett* **1984**, *52*, 1990–1993.